Atoms, dipole waves, and strongly focused light beams

S.J. van Enk
Bell Labs, Lucent Technologies
600-700 Mountain Ave, Murray Hill, NJ 07974
(Dated: February 1, 2008)

We describe the resonant interaction of an atom with a strongly focused light beam by expanding the field in multipole waves. For a classical field, or when the field is described by a coherent state, we find that both intensity pattern and photon statistics of the scattered light are fully determined by a small set of parameters. One crucial parameter is the overlap of the field with the appropriate dipole wave corresponding to the relevant dipole transition in the atom. We calculate this overlap for a particular set of strongly focused longitudinally polarized light beams, whose spot size is only $0.1\lambda^2$, as discussed in S. Quabis *et al.*, Appl. Phys. B **72**, 109 (2001).

I. INTRODUCTION

For many applications, both in classical and quantum optics, it is a good idea to focus light to a small spot size. For example, in recent experiments on single atoms trapped in tiny dipole traps [1] the focusing system plays a major role. A natural question in that context is, how strong can the interaction between a single atom in free space and a light wave be? One expects the strength of the interaction to increase with decreasing focal spot size. However, there must be an upper limit to the interaction strength for at least two reasons: first, there is a limit to how much one can focus light of a given wavelength λ; second, the cross section of a two-level atom is $\sigma = 3\lambda^2/(2\pi)$, which seems to indicate that as long as all light is focused to within σ the interaction is optimal. The latter argument, however, does not paint the complete picture. First of all, it leaves out polarization effects, and second it does not distinguish between a classical object with a cross section σ (such as a classical oscillating dipole [2]) and a quantum object with the same cross section (such as a $J = 0$ to $J = 1$ transition in an atom). Here we take a closer theoretical look at the resonant interaction of a two-level atom with strongly focused light.

To start with earlier theoretical work, in Refs. [3, 4] a standard quantum-optical version of input-output theory (see [5], and also [6]) was used to calculate the effects of light scattering off of a single atom in free space. The description of the light waves in the model has a 1-dimensional character but one may expect a full 3-dimensional calculation to be necessary if the incoming light is strongly focused. Here we show how the input-output theory can be rephrased to include the full 3-dimensional description of the input and output light beams and yet keep all characteristics of the simpler 1-dimensional model.

In other work [7, 8] on the same subject exact 3-dimensional solutions of the Maxwell equations were constructed by expanding the field in a complete set of functions that are well-suited to describe a cylindrically symmetric beam. In the present paper we use a different method, and apply the results of Refs. [9, 10], where the standard Debye approximation is used to construct exact expressions for strongly focused light beams. The authors find that a radially polarized beam of light produces a field that is longitudinally polarized in the focal spot and that is focused down to a very small spot size, namely $A \approx 0.1\lambda^2$. It is worth noting that this area is smaller than σ by almost a factor of 5.

One may wonder what the strongest focusing possible is. It turns out that that depends on one's definition. The smallest spot size is one criterion, but another, which is the most relevant for our discussion, is to find the maximum possible electric field intensity in the origin given a fixed power for an incoming beam. That maximum is known to be achieved by an electric dipole wave [11]. For illumination with a finite numerical aperture one still obtains the maximum by an electric dipole wave, but the optimum then depends on the polarization, see [12] and also Section V. In any case, a measure of how focused a given light beam is, is thus given by its overlap with the appropriate dipole wave.

Furthermore, for the interaction of light with an atom in the usual long-wavelength approximation [13], one may expand the interaction in a multipole series. To lowest order, the atom interacts through an electric dipole interaction; hence, to lowest order the only types of waves interacting with the atom are, again, electric dipole waves. Thus, it makes sense for two reasons to expand the field in multipole waves around the origin (which is where the atom is assumed to be). In addition, we note here that a multipole expansion is also convenient for the calculation of the field distribution in the focal region [14].

This paper is organized as follows: In Section II we review the essential properties of multipole waves, and in Section III we consider the interaction of an atom with a field expanded in multipole waves. In Section IV we calculate two characteristic quantities of the scattered light as functions of the location of the photodetector: one is the intensity pattern and one is the photon statistics. The former quantity is classical in some sense, as a quantum object never gives rise to an intensity pattern that cannot be also obtained from the Maxwell equations and a classical scatterer. The photon statistics, on the other hand, does provide a quantum signature of the scattering process. In Section V we consider the (longitudinally

polarized) focused light beams discussed in [9, 10] and calculate their overlap with the appropriate dipole wave. We compare the results to similar known results on transversely polarized waves. We conclude by raising several open questions concerning various aspects of focused light that are not treated in the main text.

II. MULTIPOLE WAVES

When quantizing the electromagnetic (EM) field, we may choose any complete set of mode functions to expand the electric and magnetic fields in. The usual choice is to take plane waves, but, as mentioned above, for the description of the interaction of radiation with atoms in the dipole approximation multipole waves [13] are a good alternative.

Multipole waves are eigenfunctions of commuting Hermitian operators such that the excitations of such modes (i.e., the photons) possess definite amounts of energy E [$E = \hbar\omega$], total angular momentum $\vec{J}^2$ [$\vec{J}^2 = J(J+1)\hbar^2$], angular momentum J_z in the z direction [$J_z = M\hbar$], and parity P [either $(-1)^{J+1}$ (written here as $P = X$) or $(-1)^J$ (denoted by $P = Z$)]. We thus may expand the electric and magnetic field operators as

$$\begin{aligned} \vec{E}(\vec{r}) &= \int \mathrm{d}\omega \sum_\nu \mathcal{N}_\omega \vec{\Phi}_{\omega\nu}(\vec{r}) a_{\omega\nu} + H.c. \\ c\vec{B}(\vec{r}) &= \int \mathrm{d}\omega \sum_\nu \mathcal{N}_\omega \vec{\Psi}_{\omega\nu}(\vec{r}) a_{\omega\nu} + H.c, \end{aligned} \tag{1}$$

where we abbreviated the set of discrete quantum numbers as $(J, M, P) =: \nu$ and $\sum_\nu := \sum_{J=1}^{\infty} \sum_{M=-J}^{J} \sum_{P=X}^{Z}$. Furthermore $a^\dagger_{\omega\nu}$ and $a_{\omega\nu}$ are the creation and annihilation operators for the mode with the corresponding eigenvalues ω and ν. The functions $\vec{\Phi}$ are normalized to

$$\int \mathrm{d}\vec{r} \vec{\Phi}^*_{\omega\nu}(\vec{r}) \cdot \vec{\Phi}_{\omega'\nu'}(\vec{r}) = (2\pi)^3 \delta(\omega - \omega') \delta_{\nu\nu'} \tag{2}$$

and the same for $\vec{\Psi}$. Here we used the obvious abbreviation $\delta_{\nu\nu'} = \delta_{JJ'}\delta_{MM'}\delta_{PP'}$. The normalization factor

$$\mathcal{N}_\omega = \left[\frac{\hbar\omega}{2\epsilon_0 (2\pi)^3} \right]^{1/2} \tag{3}$$

is chosen such that the free-field Hamiltonian takes the familiar form

$$\begin{aligned} H &= \frac{\epsilon_0}{2} \int \mathrm{d}\vec{r} \left[\vec{E}^2(\vec{r}) + c^2 \vec{B}^2(\vec{r}) \right] \\ &= \int \mathrm{d}\omega \hbar\omega \sum_\nu \left[a^\dagger_{\omega\nu} a_{\omega\nu} + \frac{1}{2} \right]. \end{aligned} \tag{4}$$

The expressions for the multipole waves are somewhat complicated (see [13]), but fortunately we will only need the values in the origin (which is where the atom is assumed to be), and in the far field, at a distance r from the atom with $r\omega_A/c \gg 1$ with ω_A the relevant atomic resonance frequency. In the origin, the only waves for which the electric field (with which the atom interacts to first approximation) is nonzero, are the electric dipole waves. They are the waves with quantum numbers $J = 1$ and even parity (corresponding to $P = X$). The other quantum numbers ω are arbitrary, and M takes on one of the values $M = \pm 1, 0$. In $\vec{r} = 0$ the dipole waves take on the values [13]

$$\vec{\Phi}(0)_{\omega 1 M X} = i \frac{\omega}{c^{3/2}} \left[\frac{8\pi}{3} \right]^{1/2} \hat{u}_M, \tag{5}$$

where we explicitly displayed the dipole quantum numbers $\nu = (J = 1, M, P = X)$. The unit vectors

$$\hat{u}_0 = \hat{z}; \;\; \hat{u}_{\pm 1} = (-i\hat{y} \mp \hat{x})/\sqrt{2} \tag{6}$$

are the standard unit circular vectors. In the far field, a dipole field $\vec{\Phi}_{\omega 1 M X}(\vec{r})$ reduces to [13]

$$\vec{\Phi}_{\omega 1 M X}(\vec{r}) \to i \frac{\cos(k_0 r - \pi/2)}{r} \left[\frac{6\pi}{c} \right]^{1/2} [\hat{u}_M - (\hat{u}_M \cdot \hat{r})\hat{r}], \tag{7}$$

with $k_0 = \omega/c$.

For later use it is also convenient to have the Fourier transform of a dipole wave at our disposal. It factorizes into the product of a function of the length of $\vec{k}$ and a function of the unit vector $\hat{\kappa} = \vec{k}/k$,

$$\vec{\Phi}_{k_0 1 M X}(\vec{k}) = \frac{1}{k_0} \sqrt{\frac{3}{8\pi}} \delta(k - k_0) [\hat{u}_M - (\hat{u}_M \cdot \hat{\kappa})\hat{\kappa}]. \tag{8}$$

Since we will consider (quasi-)monochromatic waves the $\hat{\kappa}$-dependent part is the most relevant for our purposes:

$$\vec{\Phi}_M(\hat{\kappa}) = \sqrt{\frac{3}{8\pi}} [\hat{u}_M - (\hat{u}_M \cdot \hat{\kappa})\hat{\kappa}], \tag{9}$$

which is normalized to

$$\int \mathrm{d}^2\hat{\kappa} |\vec{\Phi}_M(\hat{\kappa})|^2 = 1. \tag{10}$$

III. ATOM-FIELD INTERACTION

Assume we have a two-level atom with a fixed dipole moment $\vec{d} = d\hat{u}_K$, with $\hat{u}_K$ with $K = 0, \pm 1$ one of the unit circular vectors. Through the standard electric dipole coupling, $H_{\mathrm{int}} = -\vec{d} \cdot \vec{E}$, one gets the following interaction Hamiltonian in the rotating-wave approximation

$$H_{\mathrm{int}} = i\hbar \int \mathrm{d}\omega \kappa(\omega) [b^\dagger_\omega \sigma^- - \sigma^+ b_\omega], \tag{11}$$

where

$$\kappa(\omega) = |\vec{d} \cdot \vec{\phi}(0)_{\omega 1 K X}| = \left[\frac{d^2\omega^3}{6\pi^2 \hbar \epsilon_0 c^3} \right]^{1/2}. \tag{12}$$

Here we defined new creation and annihilation operators $b^\dagger_\omega$ and b_ω describing the electric dipole wave that is coupled to the atom, with quantum numbers $J = 1, M = K, P = X$ and arbitrary ω. We denote the discrete quantum numbers by $\nu = \nu_0$. Eq. (11) is the same interaction Hamiltonian as that studied in Refs.[3, 4], but its validity goes beyond a 1-dimensional model by virtue of having expanded the EM field in multipole waves, as was already mentioned before in Ref. [6].

We can now write down the Heisenberg equations of motion for atomic and field operators. The equation for $b_\omega(t)$ is easily solved to give

$$b_\omega(t) = e^{-i\omega(t-t_0)}b_0(\omega) + \kappa(\omega)\int \mathrm{d}t' e^{-i\omega(t-t')}\sigma^-(t'), \tag{13}$$

where t_0 is a time in the far past ($t_0 < t$) and $b_0(\omega) = b_\omega(t_0)$. The equations for the mode operators for all remaining modes (ω, ν) contain just the free evolution, so that

$$a_{\omega,\nu}(t) = e^{-i\omega(t-t_0)}a_0(\omega,\nu). \tag{14}$$

The standard Markov approximation now consists of assuming that $\kappa(\omega)$ is more or less constant in the relevant frequence range around the atomic frequency ω_A, and we approximate

$$\kappa(\omega) \approx \left[\frac{d^2\omega_A^3}{6\pi^2\hbar\epsilon_0 c^3}\right]^{1/2} =: \left[\frac{\Gamma}{2\pi}\right]^{1/2}, \tag{15}$$

with Γ the spontaneous emission rate constant. (Thus, one finds the same expression for Γ as in a plane-wave expansion.) Substituting this into the equations for the atomic operators gives

$$\begin{aligned}\dot\sigma^- &= -i\omega_A\sigma^- - \frac{\Gamma}{2}\sigma^- + \sqrt{\Gamma}\sigma_z b_{\rm in}(t)\\ \dot\sigma_z &= -\Gamma(1+\sigma_z) - 2\sqrt{\Gamma}\sigma^+ b_{\rm in}(t) - 2\sqrt{\Gamma}\sigma^- b^\dagger_{\rm in}(t).\end{aligned} \tag{16}$$

(The last equation also follows from $\sigma_z = 2\sigma^+\sigma^- - 1$.) Here we defined the input (justifying its name from the fact that this field drives the atom) operator [5]

$$b_{\rm in}(t) = \frac{1}{\sqrt{2\pi}}\int \mathrm{d}\omega e^{-i\omega(t-t_0)}b_0(\omega), \tag{17}$$

which satisfies the commutation relation

$$[b_{\rm in}(t), b^\dagger_{\rm in}(t')] = \delta(t-t'). \tag{18}$$

Substituting Eqs. (13) and (14) into the expansion of the electric field yields the usual separation into source and free parts, $\vec E = \vec E_{\rm free} + \vec E_{\rm source}$. In the far field

$$\vec E^{(+)}_{\rm source}(\vec r, t) \to \frac{d\omega_A^2}{4\pi\epsilon_0 c^2}\frac{\hat u_K - (\hat u_K\cdot\hat r)\hat r}{r}\sigma^-(t - r/c), \tag{19}$$

where for convenience we will only display the positive-frequency parts of the fields from now on; the negative-frequency part is just the Hermitian conjugate of the positive-frequency part, $\vec E^{(-)} = (\vec E^{(+)})^\dagger$. Causality is obeyed as the atomic operator must be evaluated at a retarded time $t - r/c$ with $r = |\vec r|$ the distance from the atom.

The free field contains two terms, one corresponding to the relevant dipole mode, the other to all remaining modes. The former depends only on the operator $b_0(\omega)$, the latter on $a_0(\omega,\nu)$, according to (again valid in the far field)

$$\begin{aligned}\vec E^{(+)}_{\rm free}(\vec r, t) \;\to\; &\int \mathrm{d}\omega b_0(\omega)e^{-i\omega(t-t_0)}\cos(kr - \pi/2)\\ &\times\left[\frac{\hbar\omega}{2\epsilon_0(2\pi)^3}\right]^{1/2}\left(\frac{6\pi}{c}\right)^{1/2} i\frac{\hat u_K - (\hat u_K\cdot\hat r)\hat r}{r}\\ &+ \sum_{\nu\neq\nu_0}\int \mathrm{d}\omega a_0(\omega,\nu)e^{-i\omega(t-t_0)}\cos(kr - J\pi/2)\\ &\times\left[\frac{\hbar\omega}{2\epsilon_0(2\pi)^3}\right]^{1/2}\left(\frac{6\pi}{c}\right)^{1/2}(i)^J\frac{\vec P_{JM}(\hat r)}{r},\end{aligned} \tag{20}$$

where $\vec P_{JM}(\hat r)$ is a transverse vector (perpendicular to $\vec r$), whose form depends only on the quantum numbers J and M, and which is a function of the unit vector $\hat r$ [13]. Again making use of a Markov approximation, we can rewrite this in terms of the input fields, evaluated at the earlier time $t - r/c$,

$$\begin{aligned}\vec E^{(+)}_{\rm free}(\vec r, t) \;\to\; &\mu b_{\rm in}(t - r/c)\frac{\hat u_K - (\hat u_K\cdot\hat r)\hat r}{r}\\ &+ \sum_{\nu\neq\nu_0}\mu a^\nu_{\rm in}(t - r/c)\frac{\vec P_{JM}(\hat r)}{r},\end{aligned} \tag{21}$$

where

$$\mu = \left[\frac{3\hbar\omega_A}{16\pi\epsilon_0 c}\right]^{1/2}. \tag{22}$$

We introduced here another set of input fields (although here these fields do not drive the atom in any way),

$$a^\nu_{\rm in}(t) = \int \mathrm{d}\omega a_0(\omega,\nu)e^{-i\omega(t-t_0)}, \tag{23}$$

with commutation relations

$$[a^\nu_{\rm in}(t), a^{\nu\dagger}_{\rm in}(t')] = \delta(t-t'). \tag{24}$$

The total field becomes then

$$\begin{aligned}\vec E^{(+)}(\vec r, t) \;\to\; &\left[\sqrt{\Gamma}\sigma^-(t - r/c) + b_{\rm in}(t - r/c)\right]\\ &\times\mu\frac{\hat u_K - (\hat u_K\cdot\hat r)\hat r}{r}\\ &+ \sum_{\nu\neq\nu_0} a^\nu_{\rm in}(t - r/c)\mu\frac{\vec P_{JM}(\hat r)}{r}\end{aligned} \tag{25}$$

In the first line one recognizes the standard expression [5, Eq. (2.22)] for the output field operator

$$b_{\rm out}(t) = b_{\rm in}(t) + \sqrt{\Gamma}\sigma^-(t). \tag{26}$$

This operator, too, satisfies

$$[b_{\rm out}(t), b^\dagger_{\rm out}(t')] = \delta(t-t'). \tag{27}$$

IV. PHOTON FLUX AND STATISTICS

In the following we suppose we measure the flux of the output field and its statistics for a fixed polarization $\hat{\epsilon}$ at some fixed position $\vec{r} = \vec{R}$ in the far field. This is not an essential assumption, and we could easily define quantities similar to the ones defined below for every polarization component detected.

It is convenient to introduce yet another input field operator

$$a_{\rm in}(t) = \frac{1}{\mathcal{P}} \sum_{\nu \neq \nu_0} a^{\nu}_{\rm in}(t) \vec{P}_{JM}(\hat{R}) \cdot \hat{\epsilon}, \tag{28}$$

where the presence of the geometric factor

$$\mathcal{P}^2 = \sum_{\nu \neq \nu_0} |\vec{P}_{JM}(\hat{R}) \cdot \hat{\epsilon}|^2 \tag{29}$$

ensures that the relation

$$[a_{\rm in}(t), a^{\dagger}_{\rm in}(t')] = \delta(t - t') \tag{30}$$

holds. Defining a similar geometric factor for the dipole field b,

$$\mathcal{D} = \hat{u}_K \cdot \hat{\epsilon} - (\hat{u}_K \cdot \hat{R})(\hat{R} \cdot \hat{\epsilon}), \tag{31}$$

the detection operator can then be compactly written in terms of the operator

$$C(t) = \mathcal{P} a_{\rm in}(t) + \mathcal{D}[b_{\rm in}(t)) + \sqrt{\Gamma}\sigma^-(t)], \tag{32}$$

with $R = |\vec{R}|$: namely, we get

$$\hat{\epsilon} \cdot \vec{E}^{(+)}(\vec{R}, t) \to \frac{\mu}{R} C(t - R/c). \tag{33}$$

We should note here that the operators appearing in C do not all commute. In particular, $b_{\rm in}(t)$ does not commute with the atomic operators, but $a_{\rm in}(t)$ does.

We can define two quantities of interest: a photon flux operator (with the dimension of a rate)

$$F = \langle C^{\dagger}(t) C(t) \rangle, \tag{34}$$

and the second-order intensity correlation function at time zero, $g^{(2)}(0)$,

$$\begin{aligned} g^{(2)}(0) &= \frac{G^{(2)}(0)}{F^2} \\ G^{(2)}(0) &= \langle C^{\dagger 2}(t) C^2(t) \rangle. \end{aligned} \tag{35}$$

The ordering of the noncommuting operators $b_{\rm in}$ and the atomic operators matters here. We can make use of a theorem given in [15] that states that in expressions such as those for F and $g^{(2)}(0)$ we can place $\vec{E}^{(+)}_{\rm source}$ to the left of $\vec{E}^{(+)}_{\rm free}$ and $\vec{E}^{(-)}_{\rm source}$ to the right of $\vec{E}^{(-)}_{\rm free}$. That is, we can place all operators $b_{\rm in}$ to the right of atomic operators and $b^{\dagger}_{\rm in}$ to the left.

This way, we can easily calculate these quantities in special cases of interest. In all cases we assume the field illuminating the atom has a central frequency ω_L with a bandwidth B sufficiently narrow so that B is smaller than other rates in the problem, $B \ll \Gamma$ and $B \ll c/R$. Often, we will be interested in the steady-state (in a frame rotating at the laser frequency ω_L) solution. Taking expectation values and moving to a frame rotating at ω_L, transforms the Heisenberg equations (16) into the optical Bloch equations

$$\begin{aligned} \langle \dot{\sigma}^- \rangle &= \big(i\Delta - \frac{\Gamma}{2}\big)\langle \sigma^- \rangle + \sqrt{\Gamma}\langle \sigma_z b_{\rm in}(t) \rangle \\ \langle \dot{\sigma}_z \rangle &= -\Gamma(1 + \langle \sigma_z \rangle) - 2\sqrt{\Gamma}\langle \sigma^+ b_{\rm in}(t) \rangle - 2\sqrt{\Gamma}\langle b^{\dagger}_{\rm in}(t) \sigma^- \rangle, \end{aligned} \tag{36}$$

where the laser detuning from resonance is $\Delta = \omega_L - \omega_A$. For later use we note that in the steady state the second equation gives

$$\sqrt{\Gamma}\big[\langle b^{\dagger}_{\rm in} \sigma^- \rangle + \langle \sigma^+ b_{\rm in} \rangle\big] + \Gamma \langle \sigma^+ \sigma^- \rangle = 0 \tag{37}$$

A. Coherent states

We are interested in the case of illumination with a field in a coherent state. One reason is that this corresponds to a laser field, another is that the statistics of the incoming light is then Poissonian, so that possible non-classical statistics arise from the scattering process, not from the incoming light.

Hence, we assume the input fields satisfy

$$\begin{aligned} b_{\rm in}(t)|\beta\rangle &= \beta \exp(-i\omega_L t)|\beta\rangle, \\ a_{\rm in}(t)|\alpha\rangle &= \alpha \exp(-i\omega_L t)|\alpha\rangle. \end{aligned} \tag{38}$$

Thus, the input field is described by just two complex amplitudes, one for the relevant dipole part, one for the rest. We also define η, a dimensionless number relating the total amplitude of the free field at the detection point to the contribution of the dipole field, as

$$\mathcal{D}\eta\beta = \mathcal{P}\alpha + \mathcal{D}\beta. \tag{39}$$

Below we will connect these quantities to the overlaps with dipole and other multipole waves. The optical Bloch equations (36) depend only on the amplitude β

$$\begin{aligned} \langle \dot{\sigma}^- \rangle &= \big(i\Delta - \frac{\Gamma}{2}\big)\langle \sigma^- \rangle + \sqrt{\Gamma}\beta\langle \sigma_z \rangle \\ \langle \dot{\sigma}_z \rangle &= -\Gamma(1 + \langle \sigma_z \rangle) - 2\sqrt{\Gamma}\beta\langle \sigma^+ \rangle - 2\sqrt{\Gamma}\beta^*\langle \sigma^- \rangle. \end{aligned} \tag{40}$$

The steady-state solution is

$$\begin{aligned} \sqrt{\Gamma}\langle \sigma^- \rangle_s &= \frac{-2\beta(1 + i\delta)}{1 + \delta^2 + 8|\beta|^2/\Gamma}, \\ \langle \sigma_z \rangle_s &= \frac{-(1 + \delta^2)}{1 + \delta^2 + 8|\beta|^2/\Gamma}, \end{aligned} \tag{41}$$

where we defined the dimensionless detuning $\delta = 2\Delta/\Gamma$. It is now straightforward to calculate the quantities F and $g^{(2)}(0)$.

First, we compare our result with that of Ref. [3, 4] for resonant excitation ($\delta = 0$). We find for the flux F

$$F \propto \frac{(1-2/|\eta|)^2 + 8|\beta|^2/\Gamma}{1+8|\beta|^2/\Gamma}. \tag{42}$$

Compare this with the expression from [4], Eq. (30),

$$F = \mathcal{R}\frac{\left(1-2\gamma_S/\gamma\right)^2 + 8\mathcal{R}\gamma_S/\gamma^2}{1+8\mathcal{R}\gamma_S/\gamma^2}, \tag{43}$$

with $\mathcal{R}$ the total incident flux, γ_S the spontaneous emission rate into the solid angle subtended by the incident beam and γ the total spontaneous emission rate (corresponding to our Γ). Extreme focusing corresponds to $\gamma_S = \gamma/2$. We can then make the identifications

$$\begin{aligned} \mathcal{R} &\leftrightarrow |\eta||\beta|^2, \\ \gamma_S/\gamma &\leftrightarrow 1/|\eta|. \end{aligned} \tag{44}$$

This comparison, though, is not perfect. In our case η is complex and can, in principle, take on any value, but $0 \le 2\gamma_S/\gamma \le 2$ (and with light coming from 1 direction only, one even has $2\gamma_S/\gamma \le 1$).

The strongest effects on photon statistics occur in the weak driving limit $|\beta|^2 \ll \Gamma$, —in the strong driving limit the atom saturates and the output field will display Poissonian statistics— and on resonance. We therefore consider the special case of weak on-resonance excitation, and obtain

$$\begin{aligned} F &= |\mathcal{D}|^2|\beta|^2|\eta-2|^2, \\ g^{(2)}(0) &= \frac{|\eta|^2|\eta-4|^2}{|\eta-2|^4}, \end{aligned} \tag{45}$$

This result of $g^{(2)}(0)$ is plotted in Figure 1. Remarkably, the plot is very similar to that obtained in Ref. [8] for illumination with Gaussian beams and detection in the forward direction (see Fig. 8 there). In the latter case, the result is plotted as a function of the beam waist. The remarkable aspect is, though, that the Gaussian beams are in fact no longer solutions to the Maxwell equations as the focusing conditions are too strong for the paraxial approximation to be valid. Here, on the other hand, the result is not an approximation, but is plotted as a function of $|\eta|$.

For reference we also give the flux of the output dipole field at position $\vec{R}$ in the *absence* of the atom: $F_0 = |\mathcal{D}\beta|^2$. This leads us to the following observations in special cases

$\eta = 1$ If one illuminates the atom with only the dipole field, so that $\eta = 1$, one has the strongest possible focusing. All light is coupled to the atom, and we note that the correspondence relation (44) shows that this case corresponds to $2\gamma_S/\gamma = 2$ in terms of Carmichael's parameters, indicating illumination with light that fills the full 4π solid angle. Moreover, this case is the only one where η and thereby the flux and photon statistics do not depend on the detection point.

For $\eta = 1$ the output flux equals the input flux: $\langle b_{\rm out}^\dagger b_{\rm out}\rangle = \langle b_{\rm in}^\dagger b_{\rm in}\rangle$, and $F = F_0$. One way to understand this is to note that while $\langle b_{\rm in}\rangle = \beta$, we have for the source field $\sqrt{\Gamma}\langle\sigma^-\rangle = -2\beta$. Thus the expectation value of the total field is $-\beta$. However, this does not mean that a π phase change is the only difference.

In fact, the statistics of the light has been affected by the presence of the atom. The output photons are bunched as $g^{(2)}(0) = 9$, even though the input field dispayed Poissonian statistics. The explanation for this effect is similar to that given in [3, 4] for strong bunching: the atom cannot absorb any photons if it is in the excited state, but can if it is in the ground state. The detection of a photon thus makes it more likely the atom would be found in the excited state, which in turn makes it more likely to detect a second photon, namely one emitted by the atom.

$\eta = 0$ When the *free* fields interfere destructively at the observation point (so that $\eta = 0$), the field there arises solely from the atom's fluorescence. That light, as is well-known, is anti-bunched and $g^{(2)}(0) = 0$ (as we are in the weak driving limit). (The reason is simple, the detection operator is $C = \mathcal{D}\sqrt{\Gamma}\sigma^-$ and applying this operator twice yields zero.) The flux F is $F = 4F_0$ as a result of the source field being twice as strong as the input dipole field, $\sqrt{\Gamma}\langle\sigma^-\rangle = -2\beta$.

$\eta \to 2$ When $\eta = 2$ one finds the largest bunching effect, with $g^{(2)}(0) \to \infty$. This occurs simply because

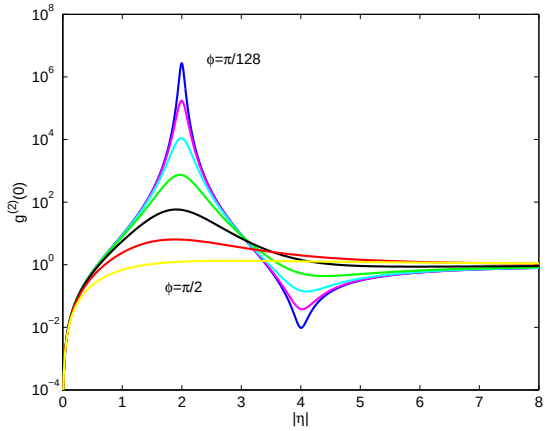

FIG. 1: $g^{(2)}(0)$, in the weak-driving limit and on resonance, as a function of $|\eta|$ for various values of the complex phase ϕ of η: $\phi = \pi/(2n)$ for $n = 1 \ldots 7$.

the total intensity there vanishes, $F \to 0$, as the source field (of amplitude -2β) destructively interferes with the free field (with dipole wave and the rest each contributing an amplitude β).

$\eta = 4$ When $\eta = 4$ the total detected flux is equal to $F = 4F_0$ with now the free fields contributing 4β to the amplitude, the source field subtracting 2β, as before. Interestingly, we again have completely anti-bunched light, $g^{(2)}(0) = 0$ (at least in the low-intensity limit). Here is why (in a quantum-trajectory picture) the light is anti-bunched in this case: The detection operator is effectively $C = \mathcal{D}(4\beta + \sqrt{\Gamma}\sigma^-)$, since the state of the free radiation field (in the detection point) is a coherent state with amplitude 4β. The steady state of the atom in between photodetection events is $|\psi\rangle = |g\rangle - 2\beta/\sqrt{\Gamma}|e\rangle$ (valid to first order order in the small parameter $\beta/\sqrt{\Gamma}$). After the first detection of a photon, we collapse the state onto $C|\psi\rangle \propto |g\rangle - 4\beta/\sqrt{\Gamma}|e\rangle =: |\phi\rangle$. The probability rate of another photon detection is proportional to the norm of the wave function $C|\phi\rangle = -16\beta^2/\sqrt{\Gamma}|e\rangle$, which is only of order $\Gamma(|\beta|^2/\Gamma)^2$. In words, the two paths to produce a photon after the first photodetection event (one from the laser field, the other from the atom) interfere almost completely destructively. Hence, $g^{(2)}(0) \to 0$ in the weak driving limit.

We note here that this type of anti-bunching is connected to a collapse of the atom to the *excited* state after the first photodetection, in contrast to the case of pure fluorescence, where the atom is collapsed into the ground state.

$\eta \to \infty$ If the field not coupled to the atom is large, the photon statistics of the total field will be dominated by that field, leading to Poissonian light with $g^{(2)}(0) \approx 1$.

V. THE DEBYE APPROXIMATION AND DIPOLE WAVES

The overlap of the incoming field with the appropriate dipole wave is clearly the most crucial quantity, as only that part interacts with the atom. For instance, if we denote that overlap by $\mathcal{O}_d$, then it easy to see that the following two relations, involving parameters used before, hold:

$$\begin{aligned} \mathcal{O}_d &= \frac{\beta}{\sqrt{|\alpha|^2 + |\beta|^2}} \\ |\eta - 1|^2 &= \frac{\mathcal{P}^2}{\mathcal{D}^2}\frac{1 - |\mathcal{O}_d|^2}{|\mathcal{O}_d|^2}. \end{aligned} \tag{46}$$

One question relevant in practice is, what is the largest overlap possible for a given numerical aperture? In order to answer this question we revert to the Debye approximation. In that approximation the field in a focus, resulting from a high numerical aperture, is expanded in plane waves (hence, the resulting expressions are conveniently given as Fourier transforms). The approximation consists in taking into account only the geometric optics rays from the aperture, thus leaving out edge effects. For a recent discussion of high-aperture beams and more background information, see [16].

In Refs [9, 10] this approximation is used to calculate the intensity profile of a particularly strongly focused type of waves that were also generated in an actual experiment. Those waves are *longitudinally* polarized in the focal spot. As before, in reciprocal space the wave function factorize into a delta function $\delta(k - k_0)$ and a part depending only on the unit vector $\hat{\kappa}$. We only need the latter part, which we denote by $\vec{\chi}$. In spherical coordinates (α, β) for $\hat{\kappa}$ one gets

$$\begin{aligned} \vec{\chi}(\alpha, \beta) &= \frac{1}{\sqrt{\mathcal{N}}} A(\alpha)\hat{p}(\alpha, \beta) \text{ for } \alpha \leq \theta \\ &= 0 \text{ otherwise,} \end{aligned} \tag{47}$$

with $\hat{p}(\alpha, \beta)$ a unit vector indicating the direction of the electric field,

$$\hat{p}(\alpha, \beta) = \begin{pmatrix} \cos\alpha\cos\beta \\ \cos\alpha\sin\beta \\ \sin\alpha. \end{pmatrix} \tag{48}$$

The previous expressions all follow directly from Eq. (9) in Ref. [10]. Here θ is related to the numerical aperture by $NA = \sin\theta$, and the normalization factor $\mathcal{N}$ is given by

$$\mathcal{N} = 2\pi \int_0^\theta \mathrm{d}\alpha \sin\alpha |A(\alpha)|^2. \tag{49}$$

The factor $A(\alpha)$ is determined by the input field on the lens. For the class of light beams studied in [9, 10],

$$A(\alpha) = \sin\alpha\sqrt{|\cos\alpha|}\exp(-a^2\sin^2\alpha), \tag{50}$$

with $a = f/w_0$ the ratio between the focal length f of the lens and the waist w_0 of the incoming Gaussian beam. The factor $\sqrt{|\cos\alpha|}$ is typical for an aplanatic lens system.

In order to determine the overlap we need the Fourier transform of the relevant dipole wave. Here we need $K = 0$ and $\vec{\Phi}_0$, since the polarization in the origin is directed along $\hat{u}_0 = \hat{z}$. From Eq. (9) we read off

$$\vec{\Phi}_0(\alpha, \beta) = \sqrt{\frac{3}{8\pi}}\sin\alpha\hat{p}(\alpha, \beta) \tag{51}$$

normalized to

$$\int_0^{2\pi} \mathrm{d}\beta \int_0^\pi \mathrm{d}\alpha \sin\alpha |\vec{\Phi}_0(\alpha, \beta)|^2 = 1. \tag{52}$$

The overlap between $\vec{\chi}$ and $\vec{\Phi}_0$ is then

$$\mathcal{O}_d = 2\pi \int_0^\theta \mathrm{d}\alpha \sin\alpha \vec{\chi}\cdot\vec{\Phi}_0 = 2\pi \int_0^\theta \mathrm{d}\alpha \sin^2\alpha A(\alpha)/\sqrt{\mathcal{N}}. \tag{53}$$

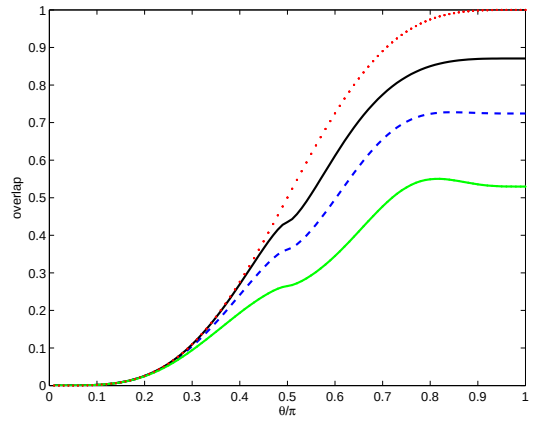

FIG. 2: Dipole wave content $p = |\mathcal{O}_d|^2$, for the longitudinally polarized waves of Eq. (50) for several values of $a = f/w_0$: the three bottom curves correspond to $a = 2, 1, 0$, respectively. The top curve gives the maximum possible overlap $|\mathcal{O}_{\max}|^2$.

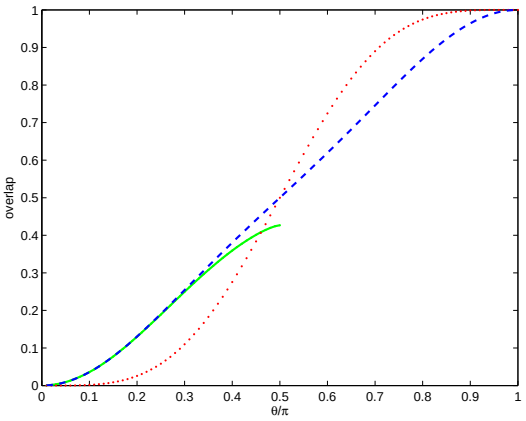

FIG. 3: Dipole wave content $p = |\mathcal{O}_d|^2$ for various waves. The dashed curve gives the maximum possible overlap with a transversely polarized electric dipole wave, obtained for a truncated dipole wave. The dotted curve gives the same but then for longitudinal polarization (and is the same dotted curve as in Fig. 2). The solid curve corresponds to uniform illumination with a transverse wave (called "Sine" wave in [12]: the result given there is valid for $\theta \leq \pi/2$). These curves are all obtained from Ref. [12].

This overlap has been calculated numerically as a function of θ, and the results are plotted in Fig. 2. The plot also shows the maximum possible overlap for given numerical aperture. That maximum is achieved when $A(\alpha) \propto \sin\alpha$. This is most easily seen by defining a scalar product

$$\langle \vec{\Phi}, \vec{\Psi} \rangle := \int_0^\theta \mathrm{d}\alpha \sin\alpha \vec{\Phi} \cdot \vec{\Psi}^*, \tag{54}$$

and noting one has to optimize this scalar product over all $\vec{\Phi}$ for fixed $\vec{\Psi} = \sin\alpha\hat{p}$. The maximum possible overlap with a dipole wave is then

$$|\mathcal{O}_{\max}|^2 = \frac{1}{2} + \frac{1}{4}\cos^3\theta - \frac{3}{4}\cos\theta. \tag{55}$$

In particular, for $\theta = \pi/2$, which corresponds to the strongest possible focusing given that the incoming light comes from one direction, one gets $|\mathcal{O}_{\max}|^2 = 1/2$, while for the types of beams considered here the best one can do is to go to the limit $a \to 0$ when $|\mathcal{O}_d|^2 = 64/147 \approx 43.5\%$.

The figure also shows that for light coming from one direction the light beams from Refs. [9, 10] are very close to the optimum (for fixed polarization) in the limit of small a, but for $\theta > \pi/2$ the distance from the optimum suddenly increases.

In most optical experiments, however, light beams in the focus are *transversely* polarized. The overlap of such beams with a transversely polarized dipole wave (in our notation, such a linearly polarized dipole wave would, of course, be a superposition of $\vec{\Phi}_1$ and $\vec{\Phi}_{-1}$), has been studied before in Refs. [11, 12]. It turns out (see Fig. 1 in [11] and Fig. 3 below) that for opening angles θ less than $\pi/2$ the overlap with the appropriate dipole waves tends to be larger for transverse than for longitudinal polarizations. This is a consequence of the latter radiation pattern having larger side lobes. This observation is true both for a truncated dipole wave and for more realistic light beams. For $\theta = \pi/2$ the dipole content of truncated dipole waves is exactly 50% for both polarizations, and for values of θ larger than $\pi/2$ longitudinally polarized waves have larger overlaps. This is plotted in Fig. 3. Let us finally compare the numbers for more realistic beams: The transversely polarized wave that results from (nearly) uniform illumination of an aplanatic lens (called "Sine" wave in [12]) has a dipole wave content $|\mathcal{O}_d|^2 = 32/75 \approx 42.7\%$ at $\theta = \pi/2$, which is in fact slightly smaller than the number quoted above for the beams described by Eq. (50) in the limit $a \to 0$.

VI. DISCUSSION

We have shown how to reformulate the quasi 1-dimensional theory of [3, 4] to study photon statistics effects in resonant light scattering off an atom in the full 3-dimensional setting, by expanding the fields in multipole waves [13]. We applied this formalism to the case of illuminating an atom with strongly focused light, and found that there is a single parameter, η, that contains all the important information. This is true when one assumes one detects a single polarization component. Otherwise, for each polarization component that is detected there is a parameter like η.

The overlap of the incoming light beam with an electric dipole wave determines the strength of the atom-light interaction. One expects that smaller focal spot sizes tend to correspond to larger overlaps, as indeed the dipole wave is the only wave with a nonzero intensity in the origin. We found a confirmation of this suspicion in Figure 2, where the overlaps of a particular class of focused

light beams with very small spot sizes are plotted. These beams turn out to have almost the maximum possible overlap, given a fixed numerical aperture (this is true within the Debye approximation), and given a *longitudinal* polarization. With this measure, the more standard case of transverse polarization leads in fact to even better focusing for opening angles θ less than $\pi/2$, although the spot sizes is actually larger [9, 10]. For $\theta > \pi/2$, on the other hand, longitudinal polarization becomes better than transverse polarization.

Finally, we note that focused light contains a great deal more structure than just a small focal spot size. In particular there are several different types of topological properties that are both robust (i.e., they do not disappear when boundary conditions are slightly changed) and generic (i.e., they occur under general, non-special circumstances). For a nice discussion see [17]. Some of those properties, such as phase and polarization singularities, occur on length scales at or even below the wavelength of the light. Similarly, around a zero of the intensity the spectral density of the light can be singular as well [18]. An open question is what the quantum signatures are of such topological structures, and whether one can probe those with an atom or a quantum dot? An atom is most likely too small to notice changes of polarization or spectrum, even if the change takes place within a wavelength, but a quantum dot may just be sufficiently large. In that case one may wonder, is there a difference between a quantum dot seeing red-shifted and blue-shifted light everywhere or seeing red-shifted light in one location and blue-shifted light in another? Or similarly, is there a difference between seeing unpolarized light or seeing horizontal polarization in one location and vertical polarization in another?

Acknowledgments

There is a whole list of people to thank for their valuable input, comments and discussions: first H.J. Kimble for many discussions on the motivation and ideas for this work, then G. Leuchs, S. Quabis, and R. Dorn for suggesting that "their" light beams may have a large overlap with dipole waves (and indeed, they do), for other discussions on focused light beams, and for their hospitality in Erlangen, and finally C.J.R. Sheppard for useful comments and for pointing out that the strongest focusing possible is achieved by (truncated) dipole waves.

[1] N. Schlosser, G. Reymond, I. Protsenko, and Ph. Grangier, Nature **411**, 1024 (2001).
[2] J.D. Jackson, *Classical electrodynamics* (Wiley, New York, 1999).
[3] H.J. Carmichael, Phys. Rev. Lett. **70**, 2273 (1993).
[4] P. Kochan and H.J. Carmichael, Phys. Rev. A **50**, 1700 (1994).
[5] C.W. Gardiner and M.J. Collett, Phys. Rev. A **31**, 3761 (1985).
[6] C.W. Gardiner, Phys. Rev. Lett. **56**, 1917 (1986).
[7] S.J. van Enk and H.J. Kimble, Phys. Rev. A **61**, 051802 (R) (2000);
[8] S.J. van Enk and H.J. Kimble, Phys. Rev. A **63**, 023809 (2001).
[9] S. Quabis, R. Dorn, M. Eberler, O. Glöckl, and G. Leuchs, Optics Comm. **179**, 1 (2000).
[10] S. Quabis, R. Dorn, M. Eberler, O. Glöckl, and G. Leuchs, Appl. Phys. B **72**, 109 (2001).
[11] C.J.R. Sheppard and P. Török, Optik **4**, 175 (1997).
[12] C.J.R. Sheppard and K.G. Larkin, J. Mod. Optics **41**, 1495 (1994).
[13] C. Cohen-Tannoudji, J. Dupont-Roc, and G. Grynberg, *Photons and Atoms*, (Wiley, New York, 1989).
[14] C.J.R. Sheppard and P. Török, J. Mod. Optics **44**, 803 (1997).
[15] W. Vogel and D.-G. Welsch, *Lectures on Quantum Optics*, (Akademie-Verlag GmbH, Berlin, 1994).
[16] C.J.R. Sheppard, J. Opt. Soc. Am. **A18**, 1579 (2001) and references therein.
[17] J.F. Nye *Natural focusing and fine structure of light: caustics and wave dislocations*, (Institute of Physics Publishing, Bristol, 1999).
[18] G. Gbur, T.D. Visser, and E. Wolf, Phys. Rev. Lett. **88**, 013901 (2002).